

PAPER

Early crystallization of amorphous selenium under high pressure studied by synchrotron XRD method



To cite this article: Shuhua Yuan *et al* 2023 *J. Phys.: Condens. Matter* **35** 264003

View the [article online](#) for updates and enhancements.

You may also like

- [Second harmonic generation from an individual amorphous selenium nanosphere](#)
C R Ma, J H Yan, Y M Wei et al.
- [Highly facile and rapid one-pot synthetic protocol for the formation of Se nanoparticles at ambient conditions with controlled phase and morphology: role of starch and cytotoxic studies](#)
Avinash Singh, Apurav Guleria, Amit Kunwar et al.
- [Modeling the radiation ionization energy and energy resolution of trigonal and amorphous selenium from first principles](#)
A Darbandi, E Devoie, O Di Matteo et al.

Early crystallization of amorphous selenium under high pressure studied by synchrotron XRD method

Shuhua Yuan^{1,2}, Luhong Wang^{3,4,*} , Fuyang Liu², Jay D Bass⁴, Yingzhe Li⁴, Paul A Ginsberg⁴, Dongzhou Zhang^{5,6}, Vitali B Prakapenka⁶, Sergey Tkachev⁶ and Haozhe Liu^{2,*} 

¹ Yangtze Delta Research Institute (Huzhou), University of Electronic Science and Technology of China, Huzhou, Zhejiang 313001, People's Republic of China

² Center for High Pressure Science & Technology Advanced Research, Haidian, Beijing 100094, People's Republic of China

³ SHARPS, Shanghai Advanced Research in Physical Sciences, Shanghai 201203, People's Republic of China

⁴ Department of Geology, University of Illinois at Urbana-Champaign, Urbana, IL 61801, United States of America

⁵ PX², Hawaii Institute of Geophysics and Planetology, University of Hawaii at Manoa, Honolulu, HI 96822, United States of America

⁶ Center for Advanced Radiation Sources, University of Chicago, Chicago, IL 60439, United States of America

E-mail: lialiu@illinois.edu and haozhe.liu@hpstar.ac.cn

Received 30 November 2022, revised 10 March 2023

Accepted for publication 29 March 2023

Published 11 April 2023



Abstract

The amorphous selenium (a-Se) was studied via x-ray diffraction (XRD) under pressures ranging from ambient pressure up to 30 GPa at room temperature to study its high-pressure behavior. Two compressional experiments on a-Se samples, with and without heat treatment, respectively, were conducted. Contrary to the previous reports that a-Se crystallized abruptly at around 12 GPa, in this work we report an early partially crystallized state at 4.9 GPa before completing the crystallization at around 9.5 GPa based on *in-situ* high pressure XRD measurements on the a-Se with 70 °C heat treatment. In comparison, crystallization pressure on another a-Se sample without thermal treatment history was observed to be 12.7 GPa, consistent with the previously reported crystallization pressure. Thus, it is proposed in this work that prior heat treatment of a-Se can result in an earlier crystallization under high pressure, which helps to understand the possible mechanism caused by the previous controversial reports on pressure induced crystallization behavior in a-Se.

Keywords: amorphous state, *in-situ* high pressure XRD, crystallization, heat treatment

(Some figures may appear in colour only in the online journal)

1. Introduction

Since its discovery in 1817, amorphous selenium (a-Se) has been one of the subjects studied extensively mainly due to its

unique atomic configurations and relevant properties [1, 2], as well as the wide technological applications in diverse industrial fields, including xerography, photovoltaics, and x-ray detectors [3]. As one of the most thoroughly studied chalcogens in the amorphous state, a-Se stands as a typical example of a monoatomic polymeric material [4, 5].

* Authors to whom any correspondence should be addressed.

Despite intensive studies in the past, there are still some controversies over the structure of a-Se [6, 7], the mechanism of crystallization [8, 9], the proportion of chain and ring structures [5, 10] and its rich pressure-induced properties, including its mechanical, electrical, optical and magnetic properties [11]. Atomic structure is crucial in determining macroscopic properties and ultimately the function of the material. Crystallized Se exists in trigonal form comprised of helical chains and monoclinic form composed of Se_8 rings in an ambient environment, and with increased temperature and pressure, it shows rich phase transitions and complex phase diagrams [12, 13]. The bulk a-Se is composed largely of uncorrelated Se_n -chains with some fraction of Se_8 rings [14], and the calculation of fraction of these molecular structures coexisting in a-Se has been quite challenging. Solving the structure in the amorphous state is more complicated than doing so for the crystalline state. To understand the structure of a-Se, many efforts have been made previously. Lucovsky *et al* [15] first reported the coexistence of 8-member rings and spiral chains via infra-red and Raman spectra, after which Nostrand reported in early 1974 that a-Se mainly consists of 8-member rings, together with a few spiral chains [1]. However, Andonov [16] and Wei [6] proposed that the tangled chains make up most of a-Se while the ring structure is the minority. Later Misawa and Suzuki [17] suggested that the structure of a-Se is not simply described as a mixture of isolated rings and chains but contains fragments characterized by both ring-like and chain-like conformations, after which Popov [18] claimed the presence of monomers in Se after performing accurate experimental measurements of the monomer content (atoms in Se_8 rings). More recently, Dash *et al* [19] proposed that a-Se, aged at room temperature, is comprised of Se_n chains and Se_8 rings.

Research work on a-Se under high pressure has also attracted lots of attention, a majority of which has been focused on pressure-induced phase transitions, including crystallization. Most of the existing literature has reported the pressure-induced crystallization from a-Se to trigonal Se where the critical pressure lies in the range of 9.7 GPa to 14 GPa [20–24]. However, more interesting observations have been reported by researchers. Liu *et al* [24] and Katayama *et al* [22] observed an unusual pressure-induced volume expansion during the crystallization. In the work of Liu *et al*, the a-Se first crystallized to a monoclinic phase which then gradually converted to the trigonal phase, and Katayama *et al* attributed this expansion to the increase of covalent bond length of a-Se under pressure. It is also worth noticing that Bridgman's experiments in 1940 displayed an anomalous phase transition of a-Se around 2.5 GPa [25–27]. Later it was proposed by Soga *et al* [28] and Singh *et al* [29] that possible inaccurate values were used in Bridgman's studies, and they reported a structural change in the glass phase at pressures around 5 GPa. Bandyopadhyay and Ming [23] have reported crystallization of a-Se from 10 GPa to 11.7 GPa according to the x-ray diffraction (XRD) measurement, which is consistent with the work of Yang *et al* [30], yet the Raman spectra indicated that the a-Se sample underwent crystallization even at the starting pressure, 0.5 GPa, which they ascribed to the laser used in the measurements. They also emphasized the possibility that the Raman

peak may be from the crystalline phase rather than from the amorphous phase, which may be due to the existence of micro-crystallization at pressures less than 10 GPa. In a more recent report by He *et al* [31], an anomalous amorphous-amorphous transition of selenium in the 2.0–2.5 GPa range was proposed based on ultrasonic and Raman spectroscopy measurements. They suggested that the anomalous compression behavior can be attributed to pressure-induced local atomic reconfiguration.

To address these controversial reports on the high pressure behavior of a-Se, an investigation of the compression behavior of two a-Se samples with different thermal histories was conducted, and the discussion about high pressure behavior of a-Se at the pressure range up to around 12 GPa is discussed in this work.

2. Methods

Two bulk samples of amorphous Se (99.999% pure) were used in this work. Sample A was heated to 70 °C before being cooled to room temperature, while sample B had been preserved at room temperature. The same *in-situ* high pressure experiments were conducted on sample A and sample B, separately. Samples were divided gently into several pieces after which a piece with dimensions around $20 \times 20 \times 30 \mu\text{m}$ was picked for compression. To form a high-pressure chamber, two well-aligned diamonds' culets with 300 μm diameter and a piece of stainless-steel gasket with 3 mm thickness were prepared. The gasket was indented to the thickness of 40 μm with these two aligned diamonds, after which a hole with 100 μm diameter was drilled by laser. Together with a thin gold foil with of size around 5 μm diameter, the chosen piece of sample was loaded into the hole that was placed between two diamond culets, then the whole chamber was loaded with helium as pressure medium and sealed with the two diamond culets. The compression of DAC with a-Se sample loaded inside was driven by the membrane gas control system. Powder XRD data were collected simultaneously while the sample was being compressed. All the powder XRD data were collected at 13BM-C, GSECARS, Advanced Photon Source, Argonne National Laboratory. Focused monochromatic beams of 0.4340 Å wavelength were used. Two-dimensional XRD patterns from both the sample and gold foil were collected and then integrated into one-dimensional patterns using the Dioptas program [32]. The XRD patterns from the gold foil were refined and thus the pressure of the chamber was calculated based on its EoS fitting.

Thermal measurements on a-Se sample from the same batch (99.999% pure) as samples A and B were carried out with a NETZSCH 404F3 thermal analyzer. To account for possible non-uniformity caused by aging or other factors, the a-Se bead was divided into several fragments, each of which weighs around 15 mg. Based on their distributions in terms of the center of the sample bead, these sample fragments were numbered #1 to #3, #1 being the outermost fragment of the sample bead, #3 the central part of the bead, and #2 being the part in between the center and outer part of the sample bead. These fragments

were heated to the temperature around 100 °C and 110 °C with a heating rate of 10 °C min⁻¹ and 30 °C min⁻¹.

3. Results and discussion

Figure 1 reports the DSC curves of the a-Se sample with a heating rate of 10 °C min⁻¹ and 30 °C min⁻¹. The sample fragments from different parts of the a-Se sample bead were used. No obvious difference in thermal performance was observed among these different fragments from the a-Se sample, which means the amorphous state is quite uniformly distributed. However, with different heating rates, the crystallization temperature varies. When the heating rate is 10 °C min⁻¹, the crystallization temperature is around 95 °C, while with a 30 °C min⁻¹ heating rate, a higher crystallization temperature at around 102 °C is observed. Explanations in line with our observation have been given by previous works [33, 34]. This observation, to some extent, supported the fact that the heat treatment helps the transition to a crystal state from amorphous state, even when the temperature in the heat treatment is much lower than the crystallizing temperature, for example, room temperature. This has been discussed as the ‘aging effect’ in other works [1, 7, 19]. In our present experiment where a-Se was heated to a temperature slightly higher than the ambient for a longer time (lower heating rate), the aging effect was more obvious, which led to a lower crystallization temperature than that with a shorter heating time (higher heating rate). Besides the large exothermic peak at around 95 °C and 102 °C indicating crystallization, we found an endothermic peak at around 50 °C and 55 °C which is the glass transition temperature. Using DSC with a heating rate of 40 °C min⁻¹, in the work of Pang *et al* [34], the thermal properties of glassy selenium quenched with various cooling rates was studied. In their work, the same endothermic peak indicating glass transition temperature was discovered at around 50 °C for samples that were quenched with cooling rates within 40 °C min⁻¹.

Before *in-situ* high pressure XRD measurement, an a-Se bulk sample (referred to sample A) was heated to 70 °C with a heating rate of 30 °C min⁻¹ using NETZSCH 404F3 thermal analyzer then cooled to room temperature. Another identical sample, referred to as sample B, had been preserved at ambient temperature, as described experimental section above. Results from XRD measurements of both sample A and sample B under pressure from ambient to over 30 GPa were shown in figures 2(a) and (b), respectively. Sample A of a-Se was heated to 70 °C before being cooled to room temperature, and exhibits an early crystallization at pressure of 4.9 GPa, which is much lower than the reported pressure for a-Se to crystallize at ambient temperature, as shown in figure 2(a). At the pressure that is lower than 4.9 GPa, XRD results of sample A do not show any obvious diffraction peaks, which means a-Se remains non-crystalline at the pressure below 4.9 GPa. Once the pressure increases to 4.9 GPa, a few main diffraction peaks of trigonal selenium start to appear, namely (101), (2-10), (2-12), (202), together with some minor diffraction peaks from monoclinic selenium structure such as (014), (231). However,

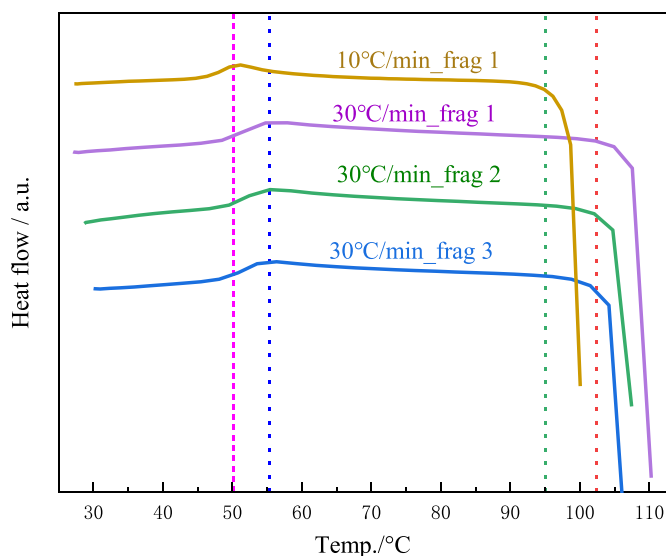


Figure 1. DSC scan of a-Se sample fragments with different heating rates.

it is worth noticing that though the diffraction peaks are obvious enough to be observed, they are not as sharp as usual. When the pressure was further increased, the diffraction peaks become sharper. The XRD patterns from sample A and sample B reveal the crystallization in a-Se sample with heat treatment, which starts from 4.9 GPa and gradually completes at 9.5 GPa, is not only gradual and slow, but also occurs unusually early under pressure. Once the pressure is increased above 9.5 GPa, a set of new diffraction peaks shows up, and more complete diffraction peaks from structures of both trigonal selenium and monoclinic selenium appear. The diffraction peaks surviving throughout the whole pressure range have been observed to shift towards the direction of a larger 2θ value, indicating the lattice of the crystallized part of the sample being compressed to a denser structure under elevated pressure.

The gradual crystallization process with a-Se were observed in earlier works done by McCann and Cartz [35] in 1972, and Gupta and Ruoff [36] in 1978, McCann and Cartz reported a slow crystallization occurred in a-Se under pressure over 6 GPa. Gupta and Ruoff observed a slow and earlier crystallization under pressure, by heating and compressing the sample simultaneously. However, Tanaka [21] showed the crystallization should be an abrupt process, and explained that the gradual crystallization in the work done by McCann and Cartz was due to the non-hydrostatic stresses in the sample chamber, which was caused by the solid pressure medium NaCl. However, in this work, where a gradual crystallization was observed starting at 4.9 GPa and completing at 9.5 GPa, the gaseous pressure medium of helium was used, which is generally considered as hydrostatic pressure medium below 12 GPa [37]. Thus, in this work, there is no evidence showing the slow crystallization in a-Se is due to non-hydrostatic environment caused by pressure medium. Instead, the abrupt crystallization observed in sample B (without heat treatment) demonstrates it is the heat treatment that result in the unusual

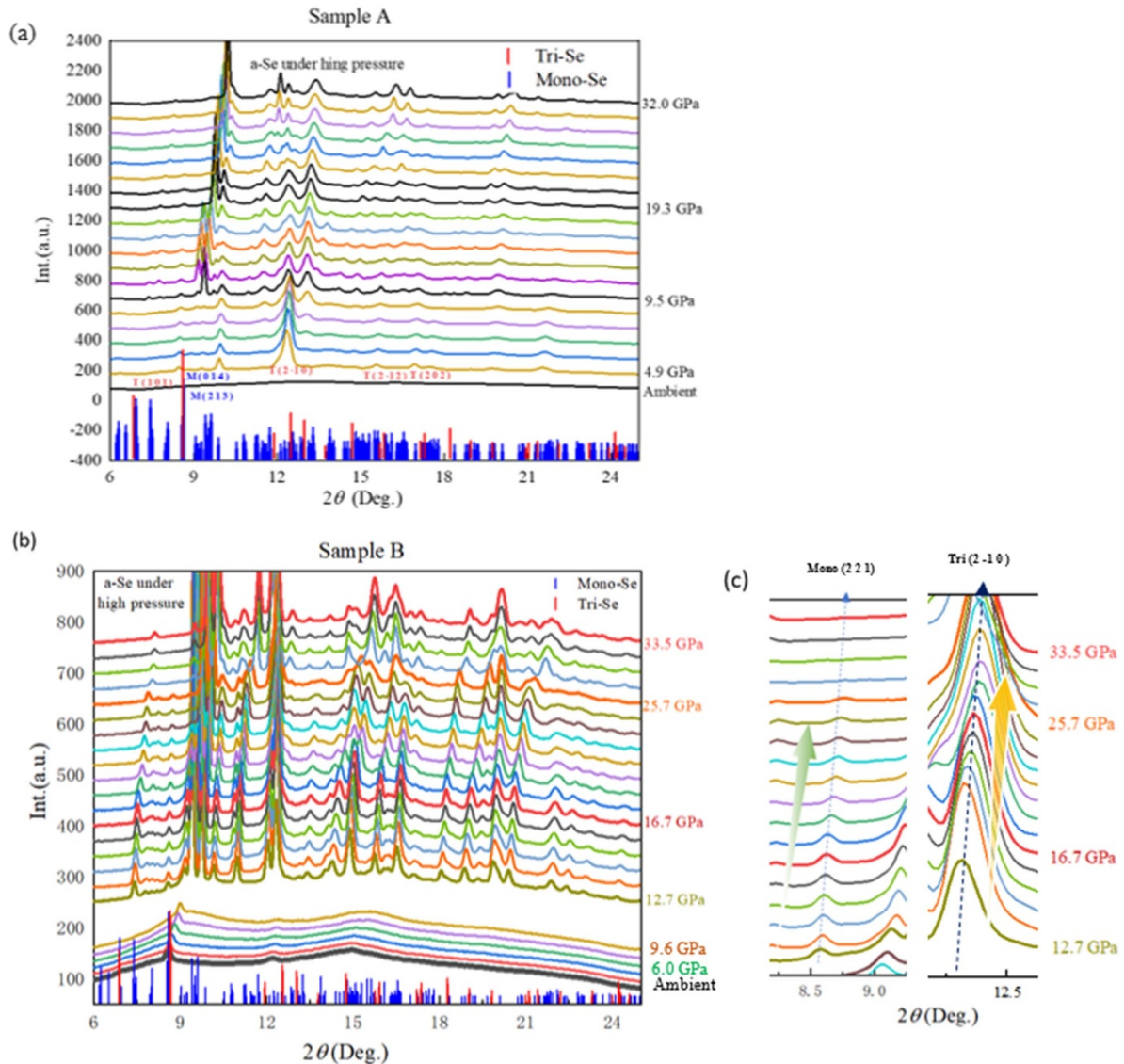


Figure 2. Typical powder x-ray diffraction data for a-Se (a) sample A with heat treatment; (b) sample B without heat treatment at increasing pressure, (c) development of selected diffraction peaks from monoclinic selenium and trigonal selenium with increasing pressure in (b). The diffraction peaks of monoclinic selenium and trigonal selenium at ambient pressure and temperature are referred from Burbank [40], Marsh *et al* [41], and Aivilov and Imamov [42].

gradual crystallization in sample A (with heat treatment). The same applies to explaining the surprisingly early crystallization observed on the a-Se sample with prior heat treatment.

As a covalent solid with two-fold coordinate, and constrained by bond-stretching forces between nearest neighbors and bond-bending-forces between next-nearest neighbors, Se has two constraints/atom [38], and the uncorrelated Se_n chains composed a flexible network. By using modulated differential scanning calorimetry examination on a-Se samples, Dash *et al* [19] obtained evidence for the existence of a growth in inter-chain structural correlations of the long super-flexible Se_n chains as a part of the aging process in a-Se. Their finding illustrates aging in a-Se sample makes chain segments in a-Se reconstruct locally to nucleate into a trigonal Se nanocrystal, and promote the growth of locally ordered Se_n chains. Se nanocrystals serve as nucleation seed sites of the trigonal

Se phase inside a-Se. For a better discussion here, we denote the state of a fresh a-Se sample as a-Se I state while the state of heat-treated a-Se sample as a-Se II state. In our present work, because a-Se (sample A) was heated to 70 °C, and the heat treatment shows a similar effect as ‘accelerated’ aging on a-Se, thus sample A evolves from a-Se I state to a-Se II state, in which the bulk sample is spatially embedded with trigonal Se nanocrystals but maintains the overall amorphous state. When the pressure is applied on sample A, which is in the state of a-Se II, the crystalline state could be easily achieved by increasing less pressure due to the nanocrystal grains throughout the bulk sample. This explains the early crystallization of a-Se under high pressure for sample A. To have more in-depth understanding with the novel crystallization process observed in a-Se with prior heat treatment, schematics of Se atomic configurations of selenium in various states and the development

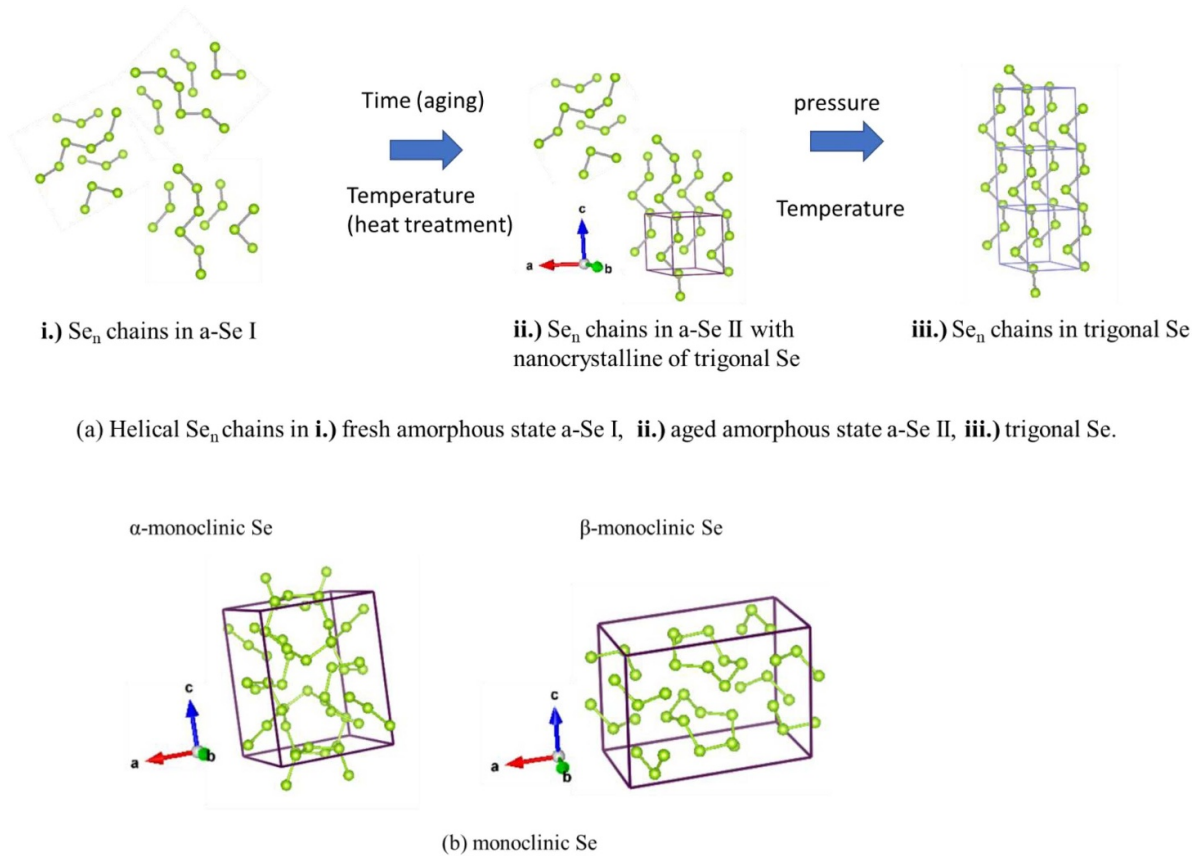


Figure 3. Schematics of Se atomic configurations in various states.

from a-Se I to a-Se II are illustrated and shown in figure 3(a) helical Se_n chains in a-Se I, a-Se II and trigonal Se, (b) α - and β -monoclinic Se with Se_8 rings.

As the counterpart of sample A, the XRD results of sample B (without heat treatment) under high pressure is presented in figure 2(b). As it is shown, the amorphous state is well maintained when the compression is less than 12.7 GPa, no sharp peaks are observed until the pressure goes to 12.7 GPa, where the crystallization happens immediately. No early crystallization is observed. Similar to the situation with sample A, for sample B, once the glassy state transforms to a crystalline state, diffraction peaks from more than one structure are observed, including trigonal selenium structure and monoclinic selenium structure, and these peaks have been coexisting throughout the investigated pressure range. With the pressure increasing from 12.7 GPa to 33.5 GPa, the diffraction peaks are not only moving towards the direction of larger 2θ value constantly, but their intensities are also varying. Many diffraction peaks have some extent overlap, and we select two typical independent diffraction peaks from trigonal and monoclinic phases which are shown in figure 2(c). With increasing pressure, the diffraction peak (2–10) from the trigonal structure gets more intensive, while the diffraction peak (221) from the monoclinic structure becomes broader and weaker. This phenomenon indicates various phases are crystallizing and growing to compete in the limited space under increasing high

pressure. Aside from the crystallization at 12.7 GPa in sample B, two other phase transitions were observed at 16.7 GPa and 25.7 GPa, respectively. This agrees with previous reports of phase transition sequences [21, 30, 39]. However, instead of crystallizing to a single trigonal phase, here we found a mixture of trigonal and monoclinic phases after the crystallization. Yang *et al* [30] proposed a direct transition from hexagonal Se I to triclinic Se III at around 19 GPa, which corresponds to phase transition at 16.7 GPa in our present work. An unknown high-pressure phase appears at 25.7 GPa, and exists together with monoclinic Se throughout the pressure range investigated in this work.

As it is mentioned in the introduction section that He *et al* [31] reported an abnormal compression behavior of a-Se in the 2.0–2.5 GPa range, and proposed a pressure-induced local atomic reconfiguration, which implies an amorphous-amorphous transition of a-Se. Although without *in situ* XRD measurement as proof, they proposed that it was an amorphous-amorphous transition induced by purely pressure, and it was ‘the third kind of transition’ described by Bridgman [25]. Combining the results from our present work here, it is noticed that more than one amorphous state could exist within a-Se. However, it is worth mentioning that none of the above studies discussed about the thermal history of the a-Se samples, or excluded the heating effect produced by laser.

4. Conclusions

In this work, *in-situ* high pressure XRD measurements on bulk a-Se samples reveal an early pressure-driven crystallization on a-Se at pressure of 4.9 GPa after a prior heat treatment of 70 °C. This unusual early crystallization is not fully completed until the pressure reaches 9.5 GPa. In comparison, for the sample without such a heat treatment, a-Se exhibits an immediate and full crystallization at high pressure of 12.7 GPa, consistent with a majority of previous reports. With increasing pressure, different pressure-induced phase transition sequences have been observed on a-Se with and without prior heat treatment. The heat treatment on a-Se has significantly changed the microstructure of a-Se, despite the lack of XRD evidence before it is compressed to 4.9 GPa. Given that temperatures near room temperature, e.g. 70 °C, could affect a-Se's microstructures, the thermal history of environmental temperature fluctuations should be considered with a-Se samples, which could explain the inconsistency among previous reports on the high pressure behavior of a-Se. This work also indicates that pressure-induced crystallization behavior could be very sensitive to possible different starting states of amorphous materials, and it is of great significance to put further effort into relevant investigations.

Data availability statement

The data cannot be made publicly available upon publication because the cost of preparing, depositing and hosting the data would be prohibitive within the terms of this research project.

Acknowledgments

This work was supported by the Natural Science Foundation of China (11374075). Portions of this work were performed at GeoSoilEnviroCARS (The University of Chicago), Advanced Photon Source (APS), Argonne National Laboratory. GeoSoilEnviroCARS is supported by the National Science Foundation—Earth Sciences (EAR—1634415) and Department of Energy—GeoSciences (DE-FG02-94ER14466). This research used resources of the Advanced Photon Source, a U.S. Department of Energy (DOE) Office of Science User Facility operated for the DOE Office of Science by Argonne National Laboratory under Contract No. DE-AC02-06CH11357.

ORCID iDs

Luhong Wang  <https://orcid.org/0000-0001-8851-4935>

Haozhe Liu  <https://orcid.org/0000-0001-5720-2031>

References

- [1] Zallen R and Lucovsky G 1974 *Selenium* ed R A Zingaro and W C Cooper (New York: Van Nostrand/Reinhold) pp 148–73
- [2] Tanaka K 2019 Amorphous selenium and nanostructures *Springer Handbook of Glass* ed J D Musgraves, J Hu and L Calvez (Cham: Springer International Publishing) pp 645–85
- [3] Huang H and Abbaszadeh S 2020 Recent developments of amorphous selenium-based x-ray detectors: a review *IEEE Sens. J.* **20** 1694–704
- [4] Hindeleh A and Johnson D 1980 An empirical estimation of Scherrer parameters for the evaluation of true crystallite size in fibrous polymers *Polymer* **21** 929–35
- [5] Yannopoulos S N 2020 Structure and photo-induced effects in elemental chalcogens: a review on Raman scattering *J. Mater. Sci., Mater. Electron.* **31** 7565–95
- [6] Wei W, Corb B W and Averbach B L 1982 A correlation model of amorphous selenium *J. Non-Cryst. Solids* **53** 19–28
- [7] Brazhkin V V and Tsiok O B 2017 Glassy selenium at high pressure: le Chatelier's principle still works *Phys. Rev. B* **96** 134111
- [8] Ye F and Lu K 1998 Pressure effect on polymorphous crystallization kinetics in amorphous selenium *Acta Mater.* **46** 5965–71
- [9] Harrison J D 1968 Seeded growth of selenium crystals under high pressure *J. Appl. Phys.* **39** 3672–5
- [10] Degtyareva O, Gregoryanz E, Somayazulu M, Dera P, Mao H-K and Hemley R J 2005 Novel chain structures in group VI elements *Nat. Mater.* **4** 152–5
- [11] Parthasarathy G and Gopal E S R 1985 Effect of high pressure on chalcogenide glasses *Bull. Mater. Sci.* **7** 271–302
- [12] Properzi L, Polian A, Munsch P and Di Cicco A 2013 Investigation of the phase diagram of selenium by means of Raman spectroscopy *High Press. Res.* **33** 35–39
- [13] Yuan S, Wang L, Zhu S-C, Liu F, Zhang D, Prakapenka V B, Tkachev S and Liu H 2022 Negative linear compressibility in Se at ultra-high pressure above 120 GPa *IUCrJ* **9** 253–60
- [14] Takumi M and Nagata K 2007 Pressure-induced phase transitions of trigonal, rhombohedral, orthorhombic, and α -monoclinic selenium *J. Phys. Soc. Japan* **76** 17–18
- [15] Lucovsky G, Mooradian A, Taylor W, Wright G B and Keezer R C 1967 Identification of the fundamental vibrational modes of trigonal, α —monoclinic and amorphous selenium *Solid State Commun.* **5** 113–7
- [16] Andonov P 1982 Studies of non-crystalline forms of selenium *J. Non-Cryst. Solids* **47** 297–339
- [17] Misawa M and Suzuki K 1978 Ring-chain transition in liquid selenium by a disordered chain model *J. Phys. Soc. Japan* **44** 1612–8
- [18] Popov A I 1976 Correlation between the molecular structure and properties of amorphous selenium *J. Phys. C: Solid State Phys.* **9** L675–7
- [19] Dash S, Chen P and Boolchand P 2017 Molecular origin of aging of pure Se glass: growth of inter-chain structural correlations, network compaction, and partial ordering *J. Chem. Phys.* **146** 224506
- [20] Shekar N V C, Yousuf M, Sahu P C, Mahendran M and Rajan K G 1993 High pressure investigations on amorphous selenium *Pramana* **40** 367–76
- [21] Tanaka K 1990 Structural studies of amorphous Se under pressure *Phys. Rev. B* **42** 11245–51
- [22] Katayama Y, Tsuji K, Shimomura O and Oyanagi H 1996 EXAFS study of amorphous selenium under pressure *J. Non-Cryst. Solids* **205–207** 199–202
- [23] Bandyopadhyay A K and Ming L C 1996 Pressure-induced phase transformations in amorphous selenium by x-ray diffraction and Raman spectroscopy *Phys. Rev. B* **54** 12049–56
- [24] Liu H, Wang L, Xiao X, De Carlo F, Feng J, Mao H-K and Hemley R J 2008 Anomalous high-pressure behavior of amorphous selenium from synchrotron x-ray diffraction and microtomography *Proc. Natl Acad. Sci.* **105** 13229–34

- [25] Bridgman P W 1940 Compressions to 50,000 kg/cm² *Phys. Rev.* **57** 237–9
- [26] Bridgman P W 1940 The compression of 46 substances to 50,000 kg/cm² *Proc. Am. Acad. Arts Sci.* **74** 21
- [27] Bridgman P W 1941 Compressions and polymorphic transitions of seventeen elements to 100,000 kg/cm² *Phys. Rev.* **60** 351–4
- [28] Soga N, Kunugi M and Ota R 1973 Elastic properties of Se and As₂Se₃ glasses under pressure and temperature *J. Phys. Chem. Solids* **34** 2143–8
- [29] Singh A K and Kennedy G C 1975 Compressibility of selenium glass to 5 GPa *J. Appl. Phys.* **46** 3861–5
- [30] Yang K *et al* 2007 Pressure-induced crystallization and phase transformation of amorphous selenium: raman spectroscopy and x-ray diffraction studies *J. Phys.: Condens. Matter* **19** 425220
- [31] He Z, Wang Z G, Zhu H Y, Liu X R, Peng J P and Hong S M 2014 High-pressure behavior of amorphous selenium from ultrasonic measurements and Raman spectroscopy *Appl. Phys. Lett.* **105** 011901
- [32] Prescher C and Prakapenka V B 2015 *DIOPTAS*: a program for reduction of two-dimensional x-ray diffraction data and data exploration *High Press. Res.* **35** 223–30
- [33] Marseglia E A and Davis E A 1982 Crystallization of amorphous selenium and As_{0.005}Se_{0.995} *J. Non-Cryst. Solids* **50** 13–21
- [34] Pang D X, Wang J T and Ding B Z 1989 Amorphous-crystalline transformation and structure in selenium *J. Non-Cryst. Solids* **107** 239–43
- [35] McCann D R and Cartz L 1972 High-pressure phase transformations in hexagonal and amorphous selenium *J. Chem. Phys.* **56** 2552–4
- [36] Gupta M C and Ruoff A L 1978 Transition in amorphous selenium under high pressure *J. Appl. Phys.* **49** 5880–4
- [37] Anderson O L, Isaak D G and Yamamoto S 1989 Anharmonicity and the equation of state for gold *J. Appl. Phys.* **65** 1534–43
- [38] Phillips J C 1979 Topology of covalent non-crystalline solids I: short-range order in chalcogenide alloys *J. Non-Cryst. Solids* **34** 153–81
- [39] Pal A, Gohil S, Sengupta S, Poswal H K, Sharma S M, Ghosh S and Ayyub P 2015 Structural phase transitions in trigonal Selenium induce the formation of a disordered phase *J. Phys.: Condens. Matter* **27** 415404
- [40] Burbank R D 1952 The crystal structure of β -monoclinic selenium *Acta Crystallogr.* **5** 236–46
- [41] Marsh R E, Pauling L and McCullough J D 1953 The crystal structure of β selenium *Acta Crystallogr.* **6** 71–75
- [42] Avilov A S and Imamov R M 1969 The structure of selenium *Sov. Phys.—Crystallogr.* **14** 330–1